TWO-PARAMETER CHARACTERIZATION OF CRACK FRONT FIELDS IN THIN DUCTILE CENTER-CRACKED GEOMETRIES

Guoyu LIN, Alfred CORNEC and Karl-Heinz SCHWALBE *

Detailed finite element analyses were carried out for 3-D crack front fields in thin ductile center-cracked panels (CCP) taking into account large geometriy changes. The applicability of the J-Q theory in 3-D geometries was carefully examined. It is shown that the near-tip fields can be represented in an alternative form in which the leading HRR-term is replaced by the standard small-scale-yielding (SSY) solution taken from the plane strain solutions of the boundary layer formulation. The evolution of crack front constraint as plastic flow progresses from small-scale yielding to fully yielded condition is examined.

INTRODUCTION

It has long been recognised that the stress triaxiality at the crack tip determines whether J-dominance is valid or not. Recently, several methods, the T-stress (Betegón and Hancock (1)) and the Q-stress (O'Dowd and Shih (2,3)) have been proposed for a second crack-tip parameter characterizing the triaxiality of the crack tip stress state.

In this paper, we discuss the extention of the two-parameter J-Q description to 3-D crack front fields in elastic-plastic material. Finite element calculations for thin center-cracked panels (CCP) loaded in tension for different crack length to specimen-width ratios a/W are carried out carefully. The solution of boundary layer formulation (BLF) in a plane strain case is defined as the reference state. In this way, the constraint parameter Q at points on a three-dimensional crack front was quantified by subtracting the reference solution scaled by J-integral from the full-field solution.

* GKSS-Research Center, Institute for Materials Research, D-21502 Geesthacht, Germany

J-Q ANNULUS

Recently, O'Dowd and Shih (2, 3) examined the character of the high and low triaxiality stress fields surrounding the finite strain zone for 2-D cracked bodies and introduced the *J-Q* annulus. They proposed the stress expansion in the angular region $|\vartheta| \leq 90°$ ahead of crack tip can be generally written as

$$\sigma_{ij}(r,\vartheta) = \sigma_{ij}^{ref}(r,\vartheta) + Q\sigma_0\delta_{ij}. \tag{1}$$

Where δ_{ij} is the kronecker delta, σ_{ij}^{ref} is a reference solution, σ_0 is the yield stress. Q is a dimensionless constant and the Q term corresponds to a hydrostatic stress . It predicts that the stress distributions with the same Q value collapse onto a single curve when the distance from the crack tip is normalized by J/σ_0.

As mentioned above, the solution from BLF for plane strain is taken as a reference state. The near-tip field of equation (1) is then approximated by

$$\sigma_{ij}(r,\vartheta) = \sigma_{ij}^{SSY}(r,\vartheta) + Q\sigma_0\delta_{ij} \tag{2}$$

Corresponding to the above definition of (2), Q is then given by matching the full field solution for $\sigma_{\vartheta\vartheta}$ with equation (2)

$$Q(z) = \frac{\sigma_{\vartheta\vartheta}(z,r,\vartheta) - \sigma_{\vartheta\vartheta}^{SSY}(r,\vartheta)}{\sigma_0} \quad \text{at } r=2J_{local}/\sigma_0,\ \vartheta=0 \tag{3}$$

NUMERICAL PROCEDURE

The geometry of specimens analyzed are center-cracked tensile panels contained a through-crack with a straight crack front. The specimen thickness $2t$ is *5mm* and crack length ratios a/W are *0.1, 0.5* and *0.9* respectively. All analyses are performed with updated Largrangian feature for more accurate description of crack-tip fields near the zone of finite strains at the crack front. The J_2 flow theory of plasticity is used in the calculations. The material response is assumed to obey the Von Mises yield criterion and the associated flow rule. The stress-strain relation under uniaxial tension follows a piece-wise power-law strain hardening as

$$\frac{\varepsilon}{\varepsilon_0} = \begin{cases} \sigma/\sigma_0 & \text{if } \sigma \leq \sigma_0, \\ (\sigma/\sigma_0)^n & \text{if } \sigma > \sigma_0, \end{cases} \tag{4}$$

where σ_0 and $\varepsilon_0 = \sigma_0/E$ are yield stress and strain, respectively and E is the Young's modulus, n is the strain hardening exponent. In the present calculations, the material constants used are poisson's ratio $\nu=0.3$, $\varepsilon_0=1/300$ and $n=10$.

RESULTS AND DISCUSSION

Fig. 1 shows the radial distribution of the hoop stress, $\sigma_{\vartheta\vartheta}$, in crack front for the crack geometry of $a/W=0.5$ under different load levels measured by $J_{av}/L\sigma_0$, where J_{av} is an average of local J over the crack front and L equal to the crack length a for $a/W=0.1$ and 0.5 and the length of uncracked ligament of $L=W-a$ for $a/W=0.9$. The stress is plotted at the mid-plane ($z/t=0.05$). The open circles indicate the SSY solution from plane strain boundary layer formulation. It can be seen that the near front fields are bounded by the SSY field. At low levels, the stresses in the center plane are close to the SSY solution. The stress level drops with increasing load level. The results for shallow and deep crack geometries, not shown here, exhibit the same features. Fig. 2 shows the radial distribution of the hoop stress, $\sigma_{\vartheta\vartheta}$, in the mid-plane ($z/t=0.05$) and the free surface ($z/t=0.96$) for crack length ratios of $a/W=0.1$, 0.5 and 0.9. The stress is plotted at a given applied level of $J_{av}/L\sigma_0=0.0048$. It can be seen that the deep and shallow crack geometries exhibit a relatively high stress triaxility. For $a/W=0.5$, the stress level drops noticeably from the mid-plane to the free surface, indicating a loss of constraint. The wide deviation of the crack front fields from the SSY fields in those various specimens suggests to make a full evaluation of a two-parameter characterization. A more detailed discussion about the constraint characterization in three-dimensional crack tip fields has been presented in (4, 5) recently.

The Q stress in the mid-plane ($z/t=0.05$) determined at different distances r from the crack-tip for $a/W=0.5$ is plotted in Fig. 3 under various applied load levels. It can be seen that Q is almost independent of r at the plotted range $r=2J/\sigma_0$ - $10J/\sigma_0$ and even for larger load level. Fig. 4 shows the radial distribution of the Q stress at different r in the mid-plane ($z/t=0.05$) and the free surface ($z/t=0.96$) for crack length ratios of $a/W=0.1$, 0.5 and 0.9. Also, Q is observed almost independent of r except for the middle crack geometry of $a/W=0.5$ at the free surface in which Q becomes weakly dependent of r.

Figs. 5 and 6 show that the distribution of Q values through the thickness at two given applied load levels $J_{av}/L\sigma_0=0.002$ and 0.0048 for $a/W=0.1$, 0.5 and 0.9, respectively. Q is evaluated at $r=2J_{local}/\sigma_0$. For shallow and deep crack geometries, the Q value is almost constant, with a sharp drop near the free surface. However, the middle crack geometry shows a more gradual drop in Q from the center to the free surface. In the mid-plane, the shallow and middle crack geometries collapse to the same value and the deep crack geometry shows a small Q value which indicates a higher triaxility at the crack front.

Fig. 7 shows the hydrostatic stress ahead of the crack front, evaluated at $r=2J_{local}/\sigma_0$, as a function of$Q$, evaluated at the same location, for different planes perpendicular to the crack front and various load levels. The a/W ratio was 0.5. It can be seen that the hydrostatic stress ahead of the crack front and the Q value has an almost linear one to one relation, which is independent of the location along the crack front and load level. The same feature is observed for the other two a/W ratios of 0.1 and 0.9.

Fig. 8 shows the dependence of local Q on the extent of plastic yielding measured by $J_{local}/L\sigma_0$ for $a/W=0.5$ at different crack front location. It shows a rapid loss of constraint near the free surface. Figs. 4, 5 and 6 show the same feature.

CONCLUDING REMARKS

The 3-D plastic in-plane fields of near-front in thin ductile center-cracked panels characterized by two parameters J and Q are demonstrated. The Q-family of fields, proposed by O'Dowd and Shih (1991,1992) for 2-D cracked bodies, continue to exist in the geometries examined. The Q values depend on the crack geometries and the load level. The deep and shallow crack geometries exhibit a higher constraint level across the thickness, while the middle crack geometry shows a quick loss of constraint at the crack front over the thickness. A linear relation between the hydrostatic stress ahead of the crack front and Q is observed, which is independent of the crack front location. Returning to Fig. 7, it seems that this relation can be characterized in the form

$$\sigma_m/\sigma_0 = \sigma_m^{SSY}/\sigma_0 + Q, \tag{5}$$

where σ_m^{SSY} is the plane strain SSY solution of the boundary layer formulation. Q characterizes the stress triaxility at the crack front.

It is intresting to note, that even in thin center cracked tensile panel, the stress state in the mid-plane is close to small scale yielding plane strain. As far as testing is concerned the most severe conditions can be achieved by using shallow or deep cracked specimens with side grooves.

SYMBOLS USED

t = specimen half-thickness (mm)

a = crack half-length (mm)

W = specimen half-width (mm)

σ_0 = uniaxial flow stress (MPa)

σ_{ij} = stress tensor (MPa)

σ_m = hydrostatic stress (MPa)

Q = local constraint factor

J_{local} = local J-Integral along crack front (N/mm)

J_{av} = average of local J through the crack front (N/mm)

n = strain hardening exponent

r, ϑ = in-plane polar coordinates

REFERENCES

(1) Betegón, C. and Hancock, J.W., J. Appl. Mech., Vol. 58, 1991, pp. 104-110.

(2) O'Dowd, N.P. and Shih, C.F., J. Mech. Phy. Solids, Vol. 39, 1991,pp. 989-1015.

(3) O'Dowd, N.P. and Shih, C.F., J. Mech. Phy. Solids, Vol. 40, 1992,pp. 939-963.

(4) Lin, G. et al. " On the two-parameter characterization of crack front fields and effect of crack constraint part I: Center-cracked geometry", Manuscript in preparation.

(5) Lin, G. et al. " On the two-parameter characterization of crack front fields and effect of crack constraint part II: Three-point bend geometry", Manuscript in preparation.

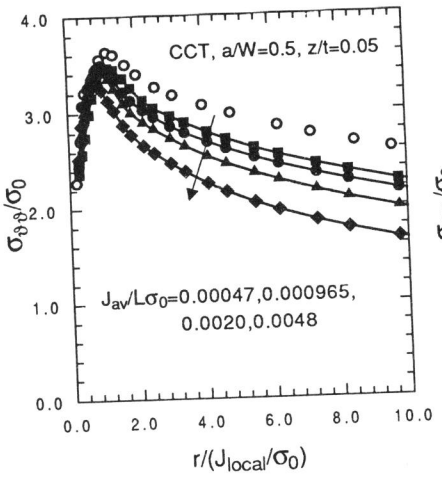

Fig.1 Normal stress in mid-plane.

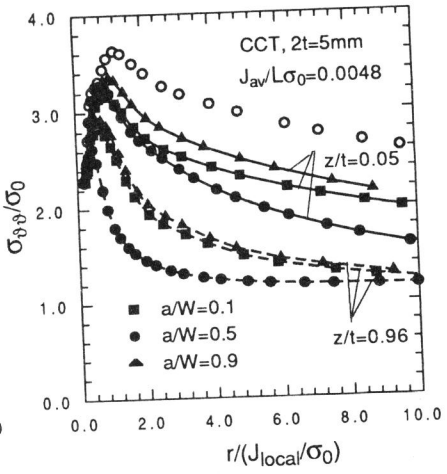

Fig.2 Normal stress in mid-plane and free surface.

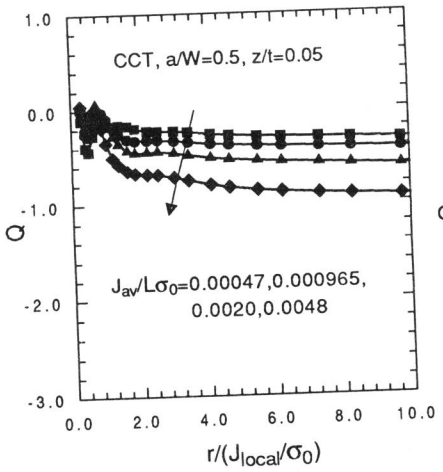

Fig.3 The Q stress field in mid-plane.

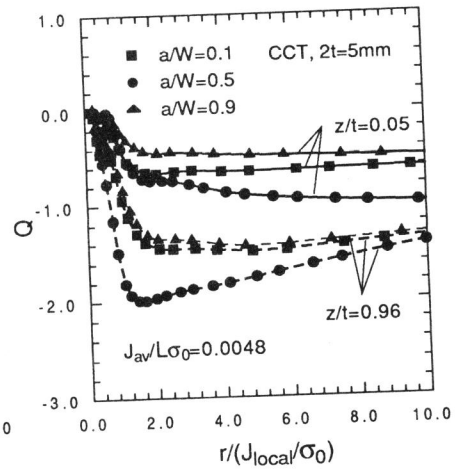

Fig.4 The Q stress field in mid-plane and free surface.

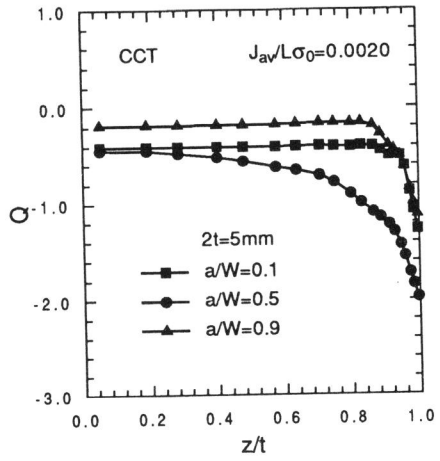

Fig.5 Q as a function of z/t in crack front at $J_{av}/L\sigma_0$=0.0020.

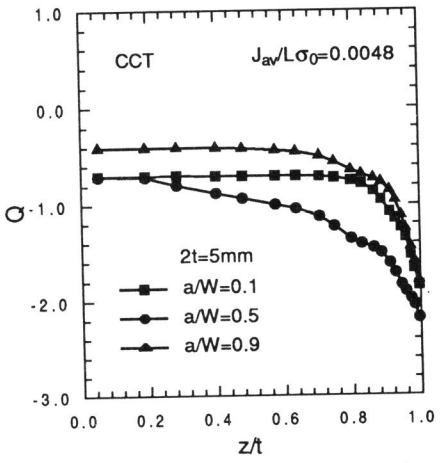

Fig.6 Q as a function of z/t in crack front at $J_{av}/L\sigma_0$=0.0048.

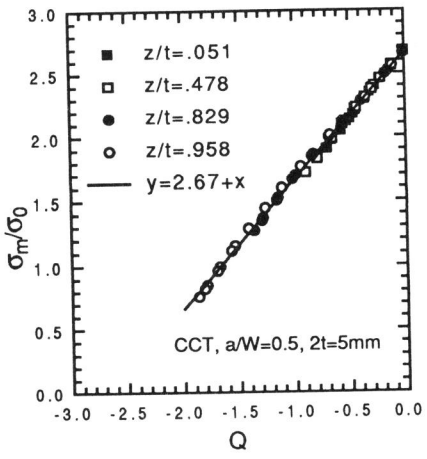

Fig.7 Q vs hydrostatic stress.

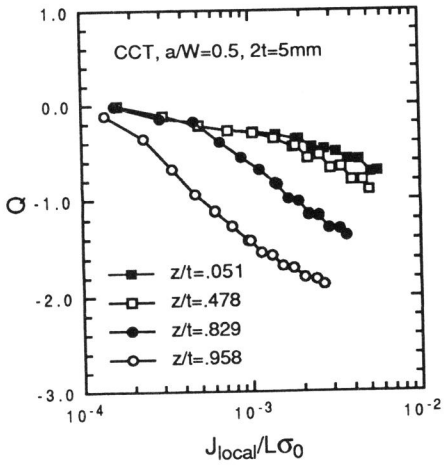

Fig.8 Variation of Q with applied load.